DESIGN OF CORELESS PCB TRANSFORMER FOR A FULL-BRIDGE DC-DC CONVERTER APPLICATION

MOHAMMADALI HASHEMI

UNIVERSITI SAINS MALAYSIA

2013

DESIGN OF CORELESS PCB TRANSFORMER FOR A FULL-BRIDGE DC-DC CONVERTER APPLICATION

by

MOHAMMADALI HASHEMI

Thesis submitted in fulfillment of the requirements
for the degree of
Master of Science

July2013

ACKNOWLEDGEMENTS

I would like to express my great gratitude to my supervisor Associate Professor Dr. Mohd Fadzil Ain for his guidance and providing me with an excellent atmosphere for doing research at Universiti Sains Malaysia.

I am also really grateful to Mohamad Ariff Bin Othman, Samiyeh Esmaeili Shaghaji, Kang Chia Chao, Olokede Sevi Stephen, Ubadullah who directly or indirectly supported me. I would like to express my great appreciation to the Universiti Sains Malaysia, Telecommunication, Electronic and PCB lab for providing equipment and helping me to complete my project.

I wish to acknowledge financial assistance provided by the Department of Electrical and Electronic Engineering, Universiti Sains Malaysia, through a Graduate Assistantship.

Moreover, I would also like to thank all of my family members for their kind support and encourage me with their best wishes.

Also, I would like to thank Universiti Sains Malaysia Research University Grant No. 1001.PELECT.814117 for supporting this research.

Thank you.

TABLE OF CONTENTS

CHAPTER FOUR : RESULTS AND DISCUSSION

CHAPTER FIVE : CONCLUSION

LIST OF TABLES

LIST OF FIGURES

Page

LIST OF SYMBOLS

Symbols	Description
R_P	Primary winding resistance
R_S	Secondary winding resistance
L_{lkp}	Leakage inductance of primary
L_{lks}	Leakage inductance of secondary
R_L	Load resistance
Cr	Resonant Capacitor
L_{mp}	Primary Mutual inductance
L_{ms}	Secondary Mutual inductance
L_m	Mutual inductance
C_{PS}	Inter-winding capacitance
L_{lk}	Leakage inductance
f	Excitation frequency
V_{dut}	Voltage across the device under test
V_{50W}	Voltage across the 50Ω resistor
R_{DC}	DC resistance of the winding
h	Height of the conductor
d	Skin depth
f	Operating frequency
m	Permeability of the medium
s	Conductivity
h_{meas}	Energy efficiency
V_{gs}	Voltage gate-source

Symbols	Description
V_{ds}	Voltage drain-source
I_g	Gate current
I_d	Drain current
C_r	Resonant capacitor
C_{GD}	Gate-drain capacitance

LIST OF ABBREVIATION

	Description
EMC	Electromagnetic compatibility
EMI	Electromagnetic interference
FR4	Flame retardant 4
CST MWS	Computer simulation technology microwave studio
MHz	Mega hertz
MIF	Maximum impedance frequency
CLPCB	Coreless printed circuit board
DC	Direct current
AC	Alternating current
MLCLPCB	Multi layered coreless printed circuit board
MOSFET	Metal oxide semiconductor field effect transistor
IGBT	Insulated gate bipolar transistor
PWM	Pulse width modulation
PCB	Printed circuit board
PSU	Power supply unit
BJT	Bipolar junction transistor
RMS	Root-mean-square
DCM	Discontinue connection mode
Tx	Transformer
RF	Radio frequency
SMPS	Switch mode power supplies
ZCS	Zero current switching
ZVS	Zero voltage switching

LIST OF PUBLICATIONS & SEMINARS

Page

REKABENTUK PENGUBAH PLT TANPA TERAS UNTUK APLIKASI PENUKAR AT-AT JAMBATAN-PENUH

ABSTRAK

Tesis ini membentangkan sebuah pengubah papan litar tercetak (PLT) tanpa teras yang dibangunkan untuk aplikasi penukar arus terus (AT) kepada (AT) jambatan-penuh. Dalam dekad yang lalu, pengubah PLT tanpa teras telah digunakan dalam aplikasi frekuensi tinggi. Telah didapati bahawa pengubah ini mempunyai ciri-ciri yang bagus dalam julat frekuensi tinggi dan tidak berguna pada frekuensi yang lebih kecil daripada 300-400 kHz. Selepas satu dekad menggunakan pengubah PLT tanpa teras disebabkan beberapa masalah seperti faktor gandingan yang rendah, kebocoran kearuhan yang tinggi dan gandaan voltan rendah, prestasi pengubah ini merosot. Objektif yang paling penting dalam tesis ini adalah pengubahsuaian reka bentuk, meningkatkan prestasi dan meningkatkan kecekapan tenaga kedua-dua pengubah PLT tanpa teras dan penukar balik AT kepada AT jambatan-penuh. Berdasarkan objektif-objektif ini, sebuah pengubah injak turun PLT tiga lapisan tanpa teras telah dipilih untuk direkabentuk dan disimulasi dengan menggunakan perisian CST Studio 3D. Pengubah ini boleh digunakan untuk kedua-dua isyarat dan pemindahan kuasa pada tahap kuasa yang rendah. Dalam kes ini, terdapat dua belitan utama dan sekunder yang dihubungkan secara siri. Di samping itu, kajian ini juga meningkatkan penukar balik AT kepada AT jambatan-penuh frekuensi tinggi dengan menggunakan peranti pensuisan kelajuan tinggi. Penukar yang telah direkabentuk beroperasi dalam julat frekuensi MHz. Dengan meningkatkan frekuensi pensuisan, komponen magnet yang besar dan sebahagian daripada alatan penukar akan dikurangkan. Julat voltan masuk bagi penukar telah diubah dari 10 – 30 V DC dengan voltan bekalan namaan sebanyak 30 V. Dalam usaha untuk meningkatkan kecekapan tenaga dan

mengurangkan kadar kehilangan, pensuisan voltan sifar (PVS) telah digunakan di dalam penukar ini. Kecekapan tenaga pengubah maksimum yang direkabentuk telah dikenal pasti sebanyak 82% pada frekuensi 1 MHz dan ia juga telah ditunjukkan bahawa kecekapan adalah lebih daripada 75% di dalam lingkungan voltan 10-30 V.

DESIGN OF CORELESS PCB TRANSFORMER FOR A FULL-BRIDGE DC-DC CONVERTER APPLICATION

ABSTRACT

This thesis present acoreless Printed Circuit Board (PCB) transformer developed for a full-bridge direct current (DC) to DC converter application. During the last decade, the coreless PCB transformer was used in high frequency applications. It was found that these transformers have good features in high frequency range and not useful at frequencies smaller than 300-400 kHz.After one decade of utilizing coreless PCB transformers due to some problems such as low coupling factor, high leakage inductance and low voltage gain, the performance of these transformers reduced. The most important objectives of this thesis are modification of the design, improve performance and increase energy efficiency of both coreless PCB transformer and full-bridge DC-DC converter. Based on these objectives, a three layer coreless PCB transformer is chosen to be designed and simulated by using CST Studio 3D software. This transformer can be employed for both signal and power transfer at low power level. In this case, there are two primary and two secondary windings that they are connected in series. In addition, this research also improves a high frequency full-bridge DC to DC converter using high speed switching devices. The designed converter operates in MHz frequency region. By increasing the switching frequency, the size of bulky magnetic components and parts of the converter is reduced. The input voltage region of converter is varied from 10-30V DC with a nominal supply voltage of 30V. In order to improve energy efficiency and reduce losses, the zero voltage switching (ZVS) technique was used in this converter. The maximum energy efficiency of the designed converter is identified to be 82% at a frequency of 1 MHz and it is also shown that the efficiency is more than 75% in the voltage range of 10-30V.

CHAPTER 1

INTRODUCTION

1.1 Background

In linear traditional power supply design a bulky power transformer typically used to provide isolation and to reduce a voltage from AC sources. The operating frequency of the power transformer applied in this power supply is at around 50/60 Hz owing to which it is heavy in weight and bulky in size. The linear power supply is regarded as an inefficient ways of transferring the signal/power from the primary side to the loads due to the losses caused by series pass elements and bulky transformer. In order to decrease losses in the bulky transformer and converter there is an increasing demand to propose a high frequency transformer for instance to reduce size, cost and weight in the converter. In this research, a coreless PCB transformer for a full-bridge DC-DC converter application is designed and developed. In this process, in order to operate at high frequency and provide suitable isolation between primary and secondary part, a high frequency transformer has been applied instead of the low frequency power transformer. In Figure 1.1 the basic block diagram which relates to the high frequency DC-DC converter is described. In this case, the DC voltage switched on and off by fast power MOSFETs is fed to the high frequency transformer as shown in Figure 1.1.

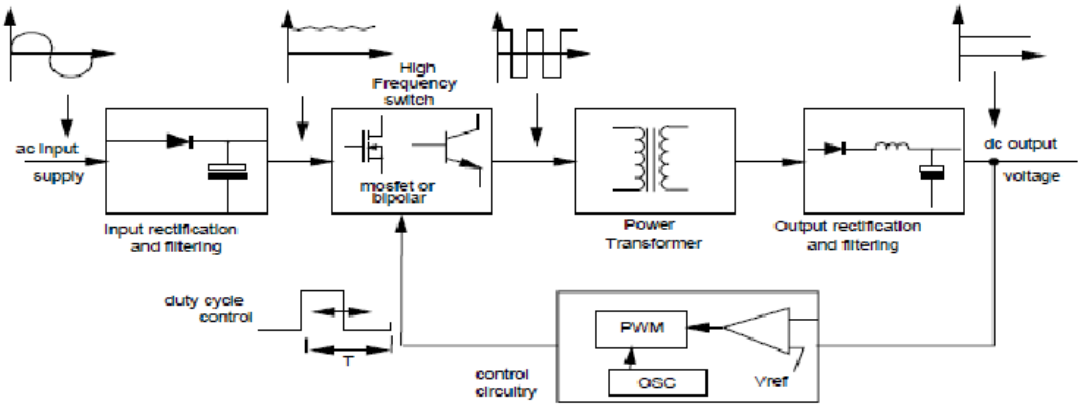

Figure 1.1: Schematic of offline switch mode power supply (SMPS) (Kotte, 2011)

This high frequency square wave signal is then fed to the primary source of the transformer and a suitable voltage magnitude which corresponds to the turn's ratio appears on the secondary side of the high frequency transformer.

1.2 Problem Statement

The factors such as compactness and high power density in power converter cause to increase the operating frequency and the use of PCB transformer. The coreless PCB transformers have great potential in applications in which space requirement and height have to be met. Moreover, the most advantages of coreless PCB transformer are given as follows: (Tang et al., 1998)

i. It has full automation and simple manufacturing process

ii. Coreless PCB transformers have good features in high-frequency operations

iii. It does not have any magnetic core, core losses and manual winding process.

iv. Primary and secondary windings of transformer can be printed on a double-sided PCB easily.

Nonetheless, after one decade of utilizing these transformers due to some problems, the performance of coreless PCB transformers reduced. The more apparent problems and challenges of coreless printed circuit board (PCB) transformers are given as follows:

i. Low coupling factor
ii. High leakage inductance
iii. Low voltage gain

In addition, challenges like having more layers and being expensive are other problems involved in multi-layer coreless PCB transformer. In addition, as frequency of the converter is increasing, consumption of the gate drive power and switching losses of the power converter are also increased.

Therefore, in this thesis the effort to improve the performance of both coreless PCB transformer and full-bridge DC-DC converter by modification of the design of previous transformers and power converters will be carried out.

1.3 Research Questions

Based on the research problem, this thesis will attempt to answer some questions such as:

1) How the coupling factor is improved?
2) How the leakage inductance is reduced?
3) How the layers of coreless PCB transformer are reduced?

4) How the design of high frequency full-bridge DC-DC converter is modified?

1.4 Research Objectives

The main objective of this research is modification of the design coreless PCB transformer for a full-bridge DC to DC converter application. In addition, the specific objectives of this thesis are given as follows:

1) To modify the design of the coreless PCB transformer for DC to DC converter application
2) To improve the performance of the coreless PCB transformer
3) To characterize the S-parameters of the coreless PCB transformer
4) To design the high frequency full-bridge DC-DC converter using coreless PCB transformer

1.5 Research Methodology

In order to achieve the objectives of this research, design of a coreless PCB transformer which is used for a full-bridge DC-DC converter application is modified and developed. At first, a novel three-layer PCB transformer is designed and simulated by using Computer Simulation Software (CST) Studio 3D software as a simulation tool, in order to characterize Scattering parameters (S-parameters) to describe electrical behavior. After the successful assessment of the coreless PCB transformer applying the simulation tool, a high speed full-bridge DC-DC converter is designed and implemented by using coreless PCB transformer. The results of this research are divided into three major parts. The first part is the simulation results of coreless PCB transformer. The second part is where the real prototype CLPCB transformer and full-bridge converter is experimented and tested for its performance. The third part is the analysis results of the proposed power converter. Finally, the conclusion Chapter gives a summary of work and also some recommendations for future works.

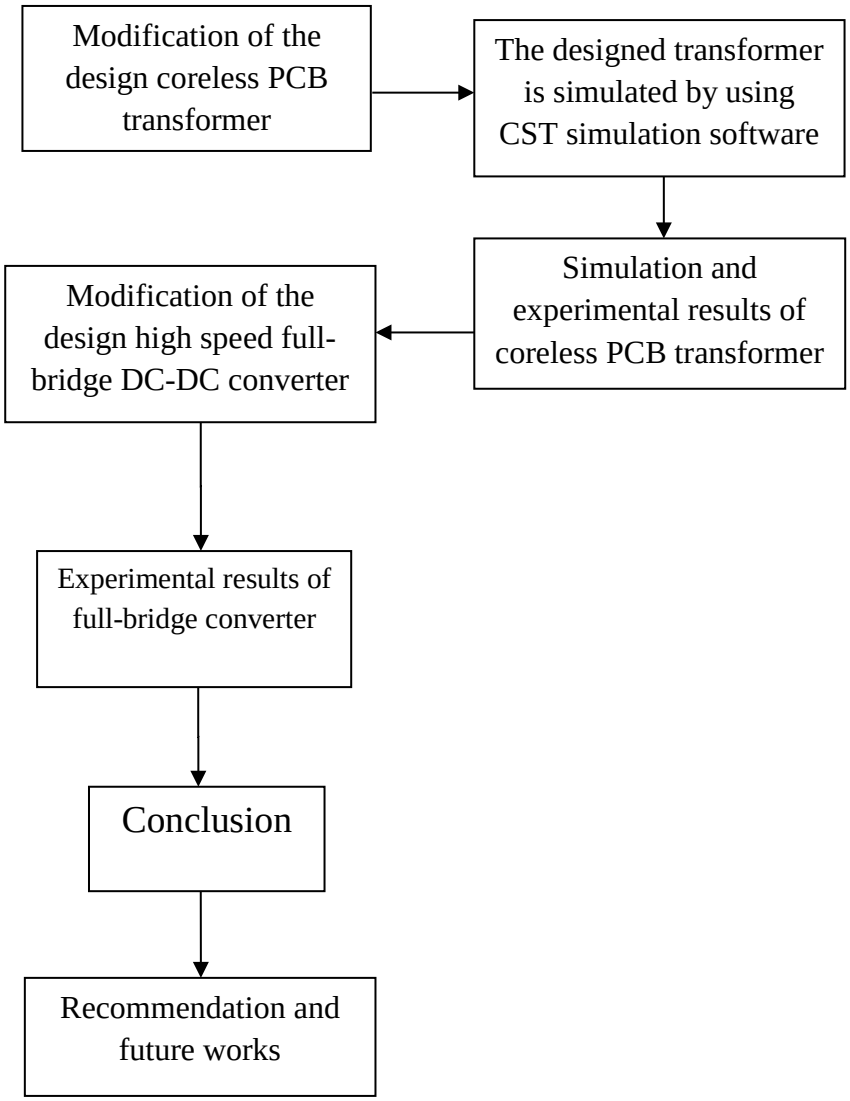

Figure 1.2: Flowchart of research methodology

1.6 Structure of Thesis

This thesis includes five chapters. The thesis is planned as follows:

Chapter 1: In this chapter, a brief introduction about advantages of coreless PCB transformer, problem statement of coreless PCB transformer, research questions, research objectives and research methodology have been presented. At the end of this chapter, research framework is given.

Chapter 2: This chapter covers literature review which is related to the multi-layered coreless PCB transformer and also high frequency DC-DC power converter. In addition, some techniques to improve energy efficiency power circuit are presented. In this chapter also a summary of previously published work is given.

Chapter 3: In this chapter the theory and design method of coreless PCB transformer and full-bridge converter in details are explained. Also, in order to develop coreless PCB transformer and full-bridge converter, some techniques are employed.

Chapter 4: This chapter presents simulation, experimental and analysis results for coreless PCB transformer and full-bridge converter. Then, all simulation, experimental and analysis results are discussed.

Chapter 5: A summary of this dissertation is given in this chapter and also suggests some area which is advantageous in improving the proposed design in the near future.

CHAPTER 2

LITERATURE REVIEW

2.1 Introduction

This Chapter revolves around the overview of the study that has been done on the coreless PCB transformer and its related literatures, which have been reviewed and consulted to achieve the objectives of this research. This Chapter will discuss about characterization of the multi-layer coreless PCB transformer and high frequency DC to DC power converter and also the employed techniques to improve energy efficiency and reduce manufacturing cost, size and losses.

2.2 Introduction Characteristics of Coreless PCB Transformer

Transformers have been proposed and generally employed over the last century; they are employed for energy transfer, signal coupling and electrical isolation. Usually, a transformer includes of copper windings wound of magnetic cores. In order to provide suitable paths for magnetic flux, ferromagnetic materials are used to make magnetic cores. They decrease the leakage inductance and provide a large degree of magnetic coupling. The operating frequency, application and power to be transferred can be considered to select the type of core in the design process. Nowadays the operating frequency of numerous switched mode power supplies has been considerably increased some hundreds kilohertz or up to few megahertz. Coreless PCB transformer consists of spiral windings which are printed on the PCB laminate. By employing printed planar windings as a replacement for twisted coil, it is possible to fabricate transformers with precise parameters.

The coreless PCB transformer includes of three parts: the primary winding, the secondary winding and the dielectric laminate. Transformer can be fabricated on the same circuit board with other electronic elements. It can also be built as a stand-alone component if desired. Coreless PCB transformers do not have limitations related with magnetic cores, for instance the frequency limitation, core losses and magnetic saturation. (S. Yipeng et al., 2012)

During the last decade, the use of PCB coils has been treated in some works. Most of them examine the planar transformers with core. Several of works study the PCB coils from different points of view. Most of the coreless PCB transformer applications given in the literature are for low output power, normally driving MOSFET transistors.

The coreless PCB transformers are not useful at frequencies smaller than 300-400 kHz, and it has good characteristics in the high frequency range from a 500 kHz to a few megahertz. Normally, at frequencies less than 300 kHz, the value of magnetizing reactance is too low, as a result current of the primary winding is too large and the voltage gain is low.

It is possible to achieve coreless PCB transformers without core with high voltage gain, high coupling factor, and low radiated EMI challenges, as will be given in this Chapter.

By using an external capacitor across the secondary winding in the PCB transformer, high voltage gain can be obtained. The external capacitor can also be achieved the resonant influence of the inductive components of the transformer and provide high voltage gain.

Exact characterization and modeling of PCB transformers is very significant for designing these transformers with electronic circuits. This Section covers features related to characterization of PCB transformers and behavior of these transformers under operating frequency and different load conditions.

A set of two different circular spiral step-down transformers which were fabricated in the four layered PCB was presented. Moreover, the coreless PCB transformers modeled with assistance of high frequency equivalent circuit. Figure 2.1 shows the high frequency equivalent circuit of transformer. (Ambatipudi., 2010)

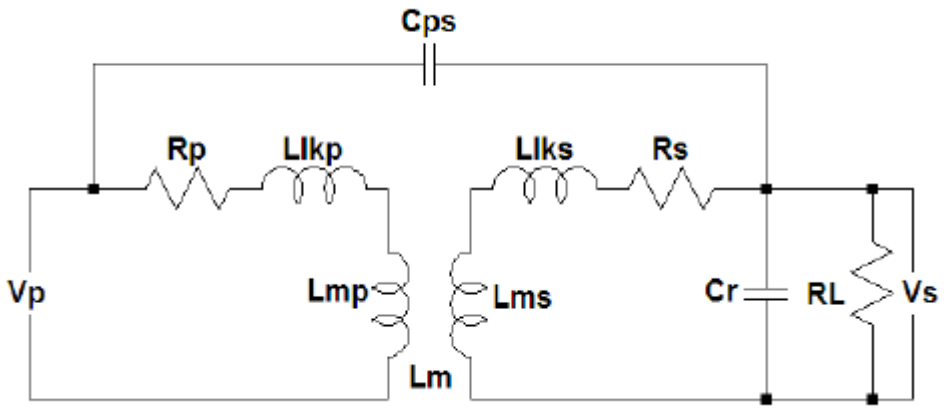

Figure 1.1: CLPCB transformer high frequency model (Ambatipudi et al., 2010)

As shown in Figure 2.1, a parallel load across the secondary winding has been employed. The electrical and initial parameters of CLPCB (Coreless PCB) transformer have been defined as follows:

R_P : Primary winding resistance;

R_S : Secondary winding resistance;

L_{lkp} : Leakage inductance of primary;

L_{lks} : Leakage inductance of secondary;

R_L : Load resistance;

Cr : Resonant Capacitor;

L_{mp} : Primary Mutual inductance;

L_{ms} : Secondary Mutual inductance;

L_m : Mutual inductance;

C_{PS} : Inter-winding capacitance;

According to high frequency equivalent circuit of transformer, parameters such as leakage and primary/secondary inductance, AC resistance, coupling coefficient, transfer function, input impedance, and resonant frequency can be obtained as follows: (Ambatipudi et al., 2010)

The transformer's leakage inductance is expressed by Equation (2.1): (Ambatipudi et al., 2010)

$$L_{lk} = \frac{50}{2\pi f}\frac{V_{dut}}{V_{50W}} \qquad (2.1)$$

Where, L_{lk} = Leakage inductance

f = Resonant frequency

V_{dut} = Voltage across the device under test

V_{50W} = Voltage across the 50 Ω resistor

And also, the primary and secondary leakage inductance of the transformer is given by (2.2) (2.3): (Hwang, 2001)

$$L_P = L_{mp} + L_{lkp} \tag{2.2}$$

$$L_S = L_{ms} + L_{lks} \tag{2.3}$$

The mutual inductance 'L_m' between the transformer's primary and secondary is the geometric mean of the primary and secondary mutual inductances 'L_{mp}'and'L_{ms}'. (Hwang and Ahn, 2001)

$$L_m = \sqrt{L_{mp} \times L_{ms}} \tag{2.4}$$

The AC resistance of the transformer is given by (2.5): (Hsu, 2005)

$$R_{AC} = \frac{R_{DC} h}{\delta(1 - \exp(-h/\delta))} \tag{2.5}$$

Where, R_{DC} = DC resistance of the winding

h = Height of the conductor

δ = Skin depth

The skin depth equation is given by equation (2.6): (Majid, 2011)

$$\delta = \frac{1}{\sqrt{\pi f \mu \sigma}} \tag{2.6}$$

Where, f = Resonant frequency

μ = Permeability of the medium

s = Conductivity

Coupling coefficient: the coupling coefficient is given by (2.7): (Erickson and Maksimović, 2001)

$$K = \frac{L_m}{\sqrt{L_p' L_S}} \tag{2.7}$$

Here, $'L_m'$ is the mutual inductance between the primary/secondary windings and $'L_P'/'L_S'$ the primary/secondary winding self-inductances.

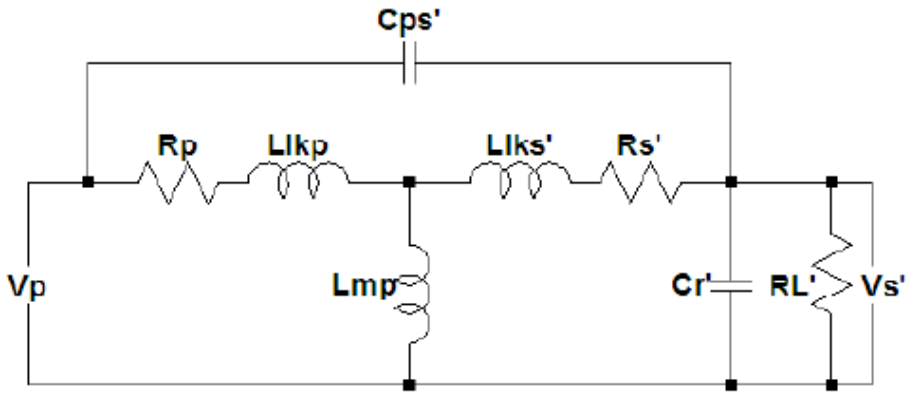

Figure 2.2: PCB transformer high frequency equivalent circuit referred to primary (Ambatipudi et al., 2010)

The related parameters such as transfer function of the coreless PCB transformer under load condition $H(f)$ and input impedance (Z_{in}) of the transformers determine the operating frequency of these transformers. According to the high frequency equivalent circuit shown in Figure 2.2 these equations are obtained as follows: (Tang et al., 2000)(S. Djuric et al., 2012)

$$H(f) = \frac{V_S}{V_P} = \frac{\frac{1}{X_1} + J(2\pi f)C_{ps}'Y_1}{nY} \tag{2.8}$$

$$Z_{in} = \frac{1}{sC_{PS}'(1 - n' \frac{V_s}{V_p}) + \frac{(1 - A)}{X_1} sC_{PP}'} \tag{2.9}$$

Here, $'n'$ is the ratio of the transformer's turn

$$R_s' = n^2 R_S \tag{2.10}$$

$$L_{lks}' = n^2 L_{lks} \tag{2.11}$$

$$C_{PP}' = C_{pp} + \frac{n - 1}{n} C_{ps} \tag{2.12}$$

$$C_r' = \frac{1}{n^2} C_r + \frac{1 - n}{n^2} C_{PS} \tag{2.13}$$

$$C_{PS}' = \frac{1}{n} C_{PS} \tag{2.14}$$

$$X_1 = R_P + sL_{lkp} \tag{2.15}$$

$$X_2 = R_S' + sL_{lks}' \tag{2.16}$$

$$Y_1 = X_2 \left[\frac{1}{X_1} + \frac{1}{sL_{mp}} \right] + 1 \tag{2.17}$$

$$Y_2 = \frac{1}{X_2} + sC_{PS}' + sC_r' + \frac{1}{n^2 R_L} \tag{2.18}$$

$$Y = - \frac{1}{X_2} + Y_1 Y_2 \tag{2.19}$$

$$A = \frac{sC_{PS}' + \frac{X_2}{X_1} Y_2}{Y} \tag{2.20}$$

Theoretically the resonant frequency of PCB transformer depends on equivalent capacitance and inductance of transformer model and is presented by the following equations: (Tang et al., 2000)

$$f_r = \frac{1}{2p\sqrt{L_{eq} \times C_{eq}}} \tag{2.21}$$

Where

$$L_{eq} = L_{lks}' + L_{mp} \| L_{lkp} \tag{2.22}$$

$$L_{eq} = L_{lks}' + \frac{L_{lkp}.L_{mp}}{L_{lks} + L_{mp}} \tag{2.23}$$

$$C_{eq} = C_r' + C_{PS}' \tag{2.24}$$

It determines that resonant frequency can be limit by equivalent capacitance and inductance of circuit model. The value of resonant capacitors across the secondary winding will play an important role in the bandwidth of the transformer. The intra-winding capacitances of transformer are very small and can be ignored.

Energy efficiency: (Sagneri et al., 2010)

$$P_{in} = \frac{1}{T}\int_0^T V_P(t) \times i_p(t)dt \tag{2.25}$$

$$P_{out} = \frac{1}{T}\int_0^T V_S(t) \times i_s(t)dt \tag{2.26}$$

Where, V_p = Instantaneous primary voltage across the primary winding

V_S = Instantaneous secondary voltage across the secondary winding

i_p = Instantaneous current through the primary winding of the transformer

i_S = Instantaneous current through the secondary winding of the transformer

T = Period of a cycle where $T = 1/f$

f = Resonant frequency of the transformer

Therefore, transformer energy efficiency can be expressed by (2.27): (Sagneri et al., 2010)

$$h_{meas} = \frac{P_{out}}{P_{in}} \times 100\% \qquad (2.27)$$

In this research, it was found while the secondary winding is sandwiched between two primary windings and also by increasing the transformer's turn number, the coupling coefficient is increased. It was proven that the coreless PCB transformers are extremely energy efficiency and can be employed in SMPS for signal/power transfer applications in MHz region. (Ambatipudi et al., 2010) (A. Bouabana et al., 2012)

2.3 Characterization of Coreless PCB Transformer

Tang (2000) presented how to characterize multilayered coreless PCB transformers. In addition, different geometrical parameters for a range of coreless transformers were evaluated. Based on an analytical process, the inductive parameters of multilayered coreless PCB transformers were calculated. It was also found that the inductance parameters of printed transformers depend on:

i. Number of turns (N);

ii. Transformer outermost radius (r);

iii. Laminate thickness (z);

iv. Conductor width (w);and

v. Conductor thickness (h).

The coreless PCB transformer was tested in the frequency range of 100 kHz to 30 MHz frequency. As a result, the measured frequency aspects indicate the inductive parameters do not varies with frequency extremely.(Tang et al., 2001a)

2.4 High Frequency DC-DC Power Converter

DC-DC Power converter is an electronic circuit which convert a source of direct current (DC) from one voltage level to another. In modern applications, factors such as power density and transient response are significant in operating of DC-DC power converters. With the increase of switching frequency of the converter, the size of the passive elements such as transformers, inductors and capacitors are reduced. These results in the increasing of energy efficiencies of the converter and power density (the amount of power) of converter can be obtained. (J. Pejtersen et al., 2012) (V. Madhuravasal et al., 2012)

2.5 Switching Form of Power MOSFET

The basic form of a switching power MOSFET consisting of a gate driver IC is described in Figure 2.3. Figure 2.3 describes the power MOSFET form including the parasitic elements for instance the drain-source, gate-source, gate-drain capacitances which all have an important effect on the switching behavior regarding switching transients.

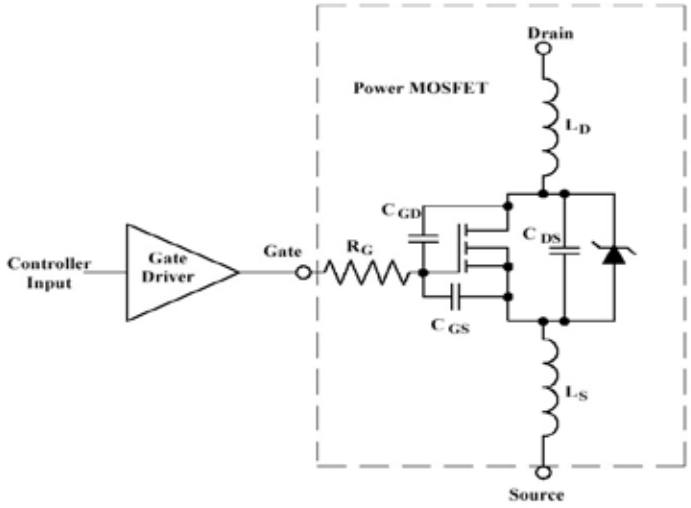

Figure 2.3: Power MOSFET switching model with the gate drive IC (Davis, July 2004)

'L_S'and'L_d' are the parasitic inductances regarding to the MOSFETs while 'R_g' is the internal resistance having a significant effect on the dv/dt of MOSFET and the switching transients. The gate-drain capacitance, 'C_{GD}' which is nonlinear regarding gate-source and drain voltages, produces the famous Miller Effect by which the MOSFET's switching speed is determined. (Balogh., 2011)

Generally, due to high capacitance at the MOSFET's gate including gate-drain 'C_{GD}' and gate-source 'C_{GS}' capacitances, high current is required to turn the device on and off.

2.6 Benefits of Raising Switching Frequency

There are different kinds of isolated converters for instance single ended and double ended topologies (fly-back and forward), half and full bridge that the main common feature of them is that their switching frequency is limited at the range between 100 kHz-1 MHz. On the other hand increasing the switching frequency of the converter has a direct effect on decreasing the passive elements size e.g.

capacitors, inductors and transformers. This increases the converter power density which brings the converter higher energy efficiencies. In addition to the mentioned benefits, as the switching converter's frequency increases the converter's closed loop response could be significantly bettered. As discussed earlier, increasing converter's switching frequency could lead to higher efficiency, compact and lightweight of the converter.

The essential switching frequency and the harmonic frequencies correspondingly which produce the electromagnetic noise, might interfere with other electronic elements in its neighborhood, for this reason the choice of switching frequency plays a significant role in this state. For instance in the situation that switching frequency is in the 530-1710 KHz range, the interference would suffer the AM radio receivers. The interference from the signal can be removed by means of a switching frequency which is beyond the frequency range of AM radio receiver. (Kotte., 2011)

2.7 Full-Bridge Converter Operation

The full bridge converter is shaped employing the four power Switches: Q1, Q2, Q3 and Q4. Figure 2.4 displays the basic configuration of a full-bridge power converter with four Switches using high frequency model of coreless PCB transformer. There are four modes of operation: (1) mode (1) when power Switches Q1 and Q4 are on, while Switches Q2 and Q3 are off; (2) mode 2 when all power Switches are off; (3) mode 3 when Q1 and Q4 are off, while Switches Q2 and Q3 are on; and (4) mode 4 when all power Switches are off. Power Switches are switched on and off consequently to provide a square wave ac at the primary side of the

transformer.The output voltage is stepped down (or up), rectified and then filtered to provide a dc voltage on output. (Muhammad., 2004)

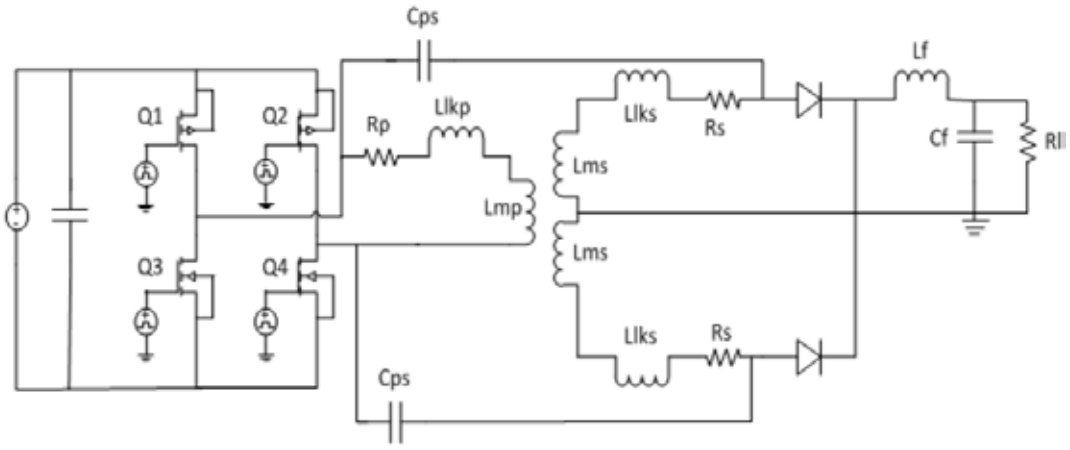

Figure 2.4: Schematic of the full bridge DC-DC converter using high frequency coreless transformer model (Saleem et al., 2011)

Mode 1. In this mode both switches Q1 and Q4 are turned on then the voltage across the secondary winding is given by equation (2.28): (Muhammad., 2004)

$$V_{se} = \frac{N_S}{N_P} V_S \tag{2.28}$$

The voltage across the output inductor *Lf* is given by (2.29): (Muhammad., 2004)

$$V_{L1} = \frac{N_S}{N_P} V_S - V_O \tag{2.29}$$

The inductor current i_{L1} increases linearly at a rate of: (Muhammad., 2004)

$$\frac{di_{Lf}}{dt} = \frac{v_{Lf}}{L_f} = \frac{1}{L_f}\left[\frac{N_S}{N_P} V_S - V_O\right] \tag{2.30}$$

Which gives the peak inductor current $I_{Lf(pk)}$ at the end of this mode at $t=kT$ as given by (2.31): (Muhammad., 2004)

$$I_{Lf(pk)} = I_{Lf}(0) + \frac{1}{L_f}\left[\frac{N_S}{N_P}V_S - V_O\right] \qquad (2.31)$$

Mode 2. This mode is valid for $kT < t \leq T/2$. In this mode all power switches are off, while D_f is forced to conduct the magnetizing current at the end of mode 1.

Mode 3 and 4. During mode 3, switches Q2 and Q3 are on, while switching devices Q1 and Q4 are off. The voltage across the primary V_P is V_S. The output voltage is given by (2.32): (Muhammad., 2004)

$$V_O = 2 \times \frac{1}{T}\left[\int_0^{kT}\left(\frac{N_S}{N_P}V_s - V_O\right)dt + \int_{T/2}^{T/2+kT} - V_O dt\right] \qquad (2.32)$$

Which gives V_O as

$$V_O = \frac{N_S}{N_P} 2V_S k \qquad (2.33)$$

The full-bridge converter is designed and used for high power applications ranging from several hundred to thousand kilowatts.

2.8 Resonant Switch:

A resonant switch is a sub-circuit including resonant elements, L_r and C_r and a semiconductor switch S. The switch S can be employed by bidirectional or unidirectional switch, which controlsthe operation mode of the resonant switch. Two forms of resonant switches, comprising zero-voltage (ZV) resonant switches and zero-current (ZC) resonant switches are displayed in Figures 2.5 and 2.6 respectively.

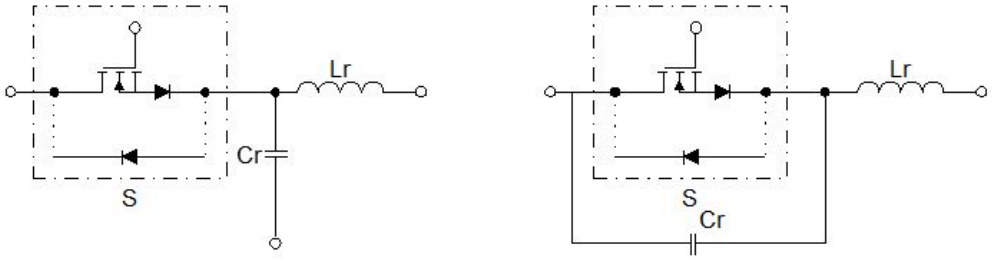

(a) (b)

Figure 2.5: Zero-voltage (ZV) resonant switch

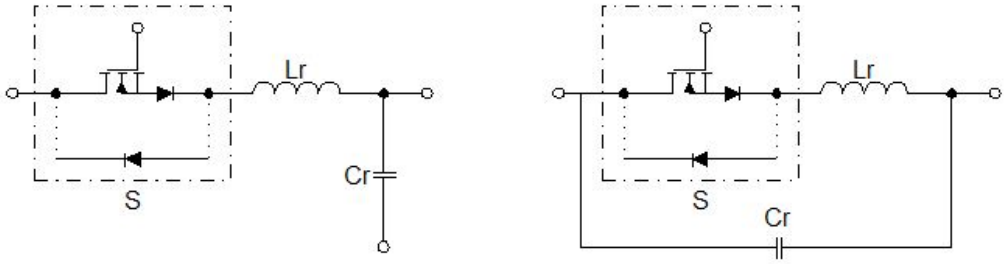

(a) (b)

Figure 2.6: Zero-current (ZV) resonant switch.

2.8.1 ZV Resonant Switch:

In a ZV resonant switch for attaining zero voltage switching (ZVS), a capacitor C_r is connected in parallel with the power switch S. The voltage across the capacitor C_r can oscillate easily in both negative and positive and half-cycle if the switch *S* is a unidirectional switch. Therefore, the resonant power switch can operate in the mode of full-wave.The resonant capacitor voltage is clamped to zero during the negative half-cycle by the diode which is connected in anti-parallel with the unidirectional power switch. The resonant power switch will then operate in the mode of half-wave. The main objective of a ZV resonant powerswitch is to employ

the resonant circuit to shape the power switch voltage waveform during the off time to provide a zero-voltage switching condition for the power switch to turn on.

2.8.2 ZC Resonant Switch

For achieving zero-current switching (ZCS) in a ZC resonant switch, an inductor L_r is connected in series with a switch S.The power switch current is permitted to resonate in the positive half cycle only if the power switch S is a unidirectional switch. The resonant power switch is said to operate in the mode of half-wave. The power switch current can flow in both directions by a diode which is connected in anti-parallel with the unidirectional power switch. Thus, the resonant power switch can operate in the mode of full-wave. The power switch current will increase gradually from zero at turn-on. Due to the resonance between C_r and L_r, it will then oscillate. Lastly, the power switch can be commutated at the next zero current duration. The main objective of this kind of switch is to shape the power switch current waveform during conduction time to provide a zero-current condition for the power switch to turn off.

2.9 S-Parameters

S-parameters (Scattering parameters) define the electrical behavior of linear electrical networks. In this Section, an introduction of S-parameters is presented. S-parameters denote the ratio between incident voltage and reflected voltage. The S-parameters are measured by sending a signal frequency into a network and detecting what waves exit from each port. Figure 2.7 shows a network with just two ports and the related s-parameters. The power, voltage, current can be considered to be in the form of waves travelling in both directions. (Franz Sischka., 2002)

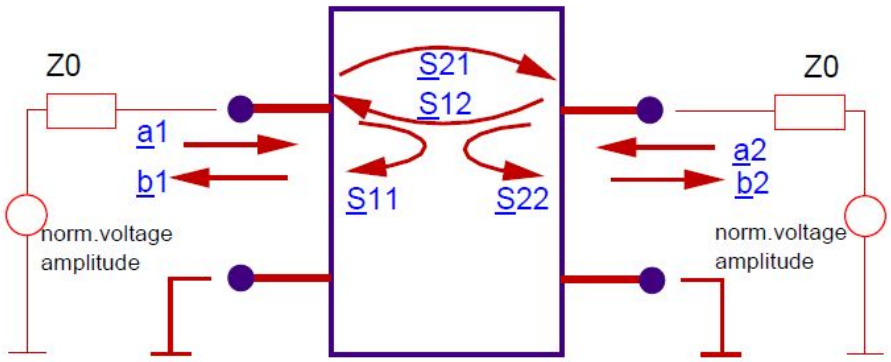

Figure 2.7: Schematic of a network with just two ports (Franz Sischka., 2002)

$$S_{11} = \frac{b_1}{a_1} \qquad S_{12} = \frac{b_1}{a_2}$$

$$S_{21} = \frac{b_2}{a_1} \qquad S_{22} = \frac{b_2}{a_2} \qquad (2.34)$$

For a wave incident on Port 1, some part of this signal reflects back out of that port and some part of the signal exits on the other ports. The parameter S_{11} refers to the power reflected from port 1. The scattering parameter S_{11} is the ratio of the two wave b1/a1. The parameter S_{11} is described is Figure 2.8. (Franz Sischka., 2002)

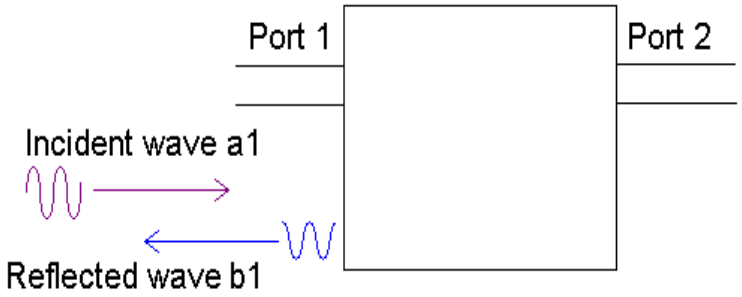

Figure 2.8: Schematic of S_{11} parameter

The parameter S_{12} refers to the power transmitted from port1 to port2. The parameter $S_{21}$is refers to the power transmitted from port2 to port1. The parameter